Oxygen dependence of photosynthesis and light-enhanced dark respiration studied by High-Resolution PhotoRespirometry

BACHELOR'S THESIS

In partial fulfillment of the requirements for the degree

„Bachelor of Science in Engineering"

Bachelor Program:

„Biotechnology and Food Engineering"

Management Center Innsbruck

Internal Supervisor:

Dr. Alexander Trockenbacher

Supervisor:

Ao. Univ.-Prof. Dr. Erich Gnaiger

Verfasser/Verfasserin:

Nora Went

01540802

Declaration in lieu of oath

I hereby declare, under oath, that this bachelor thesis has been my independent work and has not been aided with any prohibited means. I declare, to the best of my knowledge and belief, that all passages taken from published and unpublished sources or documents have been reproduced whether as original, slightly changed or in thought, have been mentioned as such at the corresponding places of the thesis, by citation, where the extent of the original quotes is indicated.

The paper has not been submitted for evaluation to another examination authority or has been published in this form or another.

Innsbruck, 2021-05-28

_____

First name/surname

Acknowledgement

Abstract

The bioenergetic crosstalk between mitochondria and chloroplasts plays a key role in maintaining metabolic integrity and controlling metabolite production for growth and regulation of cell concentration. Dark respiration and photosynthesis were studied in the green alga *Chlamydomonas reinhardtii* at varying oxygen concentrations and three cell concentrations. Light-enhanced dark respiration *LEDR* was measured after light-dark transitions (Shimakawa et al. 2020). Algae were grown photoautotrophically at 25 °C and a light intensity of 100 µmol·s^{-1}·m^{-2}. High-resolution respirometry based on the Oroboros O2k is extensively applied to the study of mitochondrial physiology in the biomedical field (Doerrier et al. 2018; Gnaiger 2020). Real-time net O$_2$ production rate (net photosynthesis *NP*) was measured with the NextGen-O2k. Light intensities (blue) were controlled with the O2k-PhotoBiology-Module in the range from 0 to 350 µmol·s^{-1}·m^{-2}. Dark respiration *DR*– determined initially at normoxia– was independent of cell concentration when expressed as O$_2$ flow per cell. At stepwise increments of light intensity *NP* was stimulated to a maximum while O$_2$ concentration increased from 220 µM to 350 up to 650 µM depending on cell count per volume in the closed reaction chamber. Alternatively, O$_2$ concentration was prevented from reaching severe hyperoxia by intermittent downregulation of O$_2$ concentration in the chamber. Independent of cell concentration, *NP* was inhibited gradually from normoxia to severe hyperoxia by up to 40 %. *LEDR* was a sharp (negative) maximum of respiration at approximately 30-60 s after light-dark transitions, increasing 3- to 4-fold compared to *DR*. No O$_2$ dependence could be assigned to *LEDR* measured at normoxia and hyperoxia. Taken together, the present results indicate that the decline of net O$_2$ production under hyperoxia was not caused by compensatory light-enhanced photorespiration *LEPR*, if *LEDR* is proportional to *LEPR* (Shimakawa et al. 2020), but was due to inhibition of photosynthesis at high O$_2$ concentrations.

Kurzfassung

Der gegenseitige, bioenergetische Einfluss zwischen Mitochondrien und Chloroplasten stellt eine Schlüsselrolle für die Aufrechterhaltung eines intakten Zellstoffwechsels dar sowie für die Regulierung von Stoffwechselprodukten für Zellwachstum und Zellzahl. Die sogenannte Dunkelatmung und Photosynthese wurden in der Grünalge *Chlamydomonas reinhardtii* bei variierenden Sauerstoffkonzentrationen und drei verschiedenen Zellzahlkonzentration im Rahmen der vorliegenden Bachelorarbeit untersucht. Durch Licht erhöhte Dunkelatmung *LEDR* wurde nach Übergängen von Belichtungs- zu Dunkelphasen gemessen (Shimakawa et al. 2020). Die Algenkultur wurde photoautotroph bei einer Temperatur von 25 °C und einer Lichtintensität von 100 µmol·s^{-1}·m^{-2} inkubiert. Die hochauflösende Respirometrie basierend auf dem Oroboros O2k wird extensiv im biomedizinischen Forschungsbereich der mitochondrialen Physiologie angewendet (Doerrier et al. 2018; Gnaiger 2020). Echtzeitmessungen von Sauerstoffproduktionsraten (netto Photosyntheserate *NP*) erfolgten anhand des NextGen-O2k. Lichtintensitäten wurden mittels des O2k-PhotoBiologie-Moduls im Bereich von 0 bis 350 µmol·s^{-1}·m^{-2} kontrolliert. Die Dunkelatmung *DR*, welche zu Beginn der Versuche bei Normoxie jeweils bestimmt wurde, war unabhängig von der Zellkonzentration. *DR* wurde als Sauerstofffluss pro Zelle ausgedrückt. Bei schrittweiser Steigerung der Lichtintensitäten wurde *NP* auf ein Maximum stimuliert, wobei Sauerstoffkonzentrationen von 220 µM auf 350 µM bis auf 650 µM anstiegen, abhängig von der Zellkonzentration innerhalb der geschlossenen Reaktionskammer. Alternativ dazu wurden Sauerstoffkonzentrationen durch wiederholtes Öffnen der Reaktionskammern reduziert und Hyperoxie vermieden. Unabhängig von Zellkonzentration wurde *NP* sukzessiv von Normoxie bis zu ausgeprägter Hyperoxie um bis zu 40 % inhibiert. *LEDR* wurde als scharfes (negatives) Maximum der Zellatmung innerhalb von 30 bis 60 s nach dem Wechsel von Licht- auf Dunkelphasen verzeichnet. Dabei wurde *LEDR* verglichen mit *DR* um das 3- bis 4-fache verstärkt und wies keine Sauerstoffabhängigkeit auf. Kombiniert deuten die Ergebnisse darauf hin, dass die Abnahme von *NP* bei Hyperoxie durch Photoinhibition bei hohen Sauerstoffkonzentrationen erfolgte und nicht durch eine kompensierende erhöhte Zellatmung *LEPR* verursacht wurde (Shimakawa et al. 2020).

Inhaltsverzeichnis

Introduction

This thesis is the extended version of the preprint "Oxygen dependence of photosynthesis and light-enhanced dark respiration studied by High-Resolution PhotoRespirometry" with a more detailed approach (Went et al. 2021). Under the framework of the H2020 EIC-SMEInst-2018-2020 NextGen-O2k project, sponsored by the European Union, this study is contributing to the market release of the NextGen-O2k, the next generation of the O2k core technology in High-Resolution Respirometry of Oroboros Instruments. In addition to the prior developed O2k-FluoRespirometer, amongst several new features the O2k-PhotoBiology-Module (PB-Module) was integrated for the conduction of oxygen (O_2) production measurements and other bioenergentic parameters at different light intensities. This innovation is targeting fields in algal biotechnology and environmental physiology. The results gained through this thesis demonstrate the possible exploitation of the NextGen-O2k for O_2 evolving mechanisms coupled to illumination. The PB-Module facilitates the physiological characterization of different algal species as the NextGen-O2k simultaneously measures O_2 consumption and production both involved in metabolic pathways in response to changing light intensities (Doerrier et al. 2021).

Biotechnological advances are proving the necessity of the utilization of biological processes, such as photosynthesis, for alternative energy production addressing energy supply in a time of global warming (Melis 2007; Scoma et al. 2014; Nagy et al. 2018). In order to exploit photosynthesis, a better understanding of its association with respiration is needed (Shimakawa et al. 2020). In this study, the crosstalk of chloroplasts and mitochondria was examined by investigating the rate of dark respiration *DR* and of net photosynthesis *NP* at varying light intensities in the range of 0 to 350 µmol photons $m^{-2} s^{-1}$ and after light-dark transitions at three cell concentrations of the green alga *Chlamydomonas reinhardtii*.

Chlamydomonas reinhardtii

The unicellular alga *Chlamydomonas reinhardtii* is a widely used model organism due to its well-known genetic properties (Rochaix 1995; Harris 2001). It can grow autotrophically, mixotrophically and

heterotrophically. The oval shaped cells measure a length of 10 μm and a width of 3 μm with two flagellae. 40 % of the cell volume consists of one chloroplast and multiple mitochondria (Rochaix 2014). The organism gained importance with the development of methods in the field of nuclear and chloroplast transformation, creating an opportunity to examine the chloroplast-mitochondrial interactions that are of the interest in this study (Rochaix 1995). Thus, this microalga was well fitted for this study.

Interactions of chloroplasts and mitochondria

Both cell organelles, mitochondria and chloroplasts, possess similar features in terms of ATP synthesis by translocating protons (H^+) by a proton motive force initiated by electron transfer in enzymatic Complexes to provide energy to the cell (Campbell and Reece 2005). In algal mitochondria, two types of pathways are known following coenzyme Q (Finnegan et al. 2004; Millar et al. 2011). One pathway transfers electrons from coenzyme Q to cytochrome c oxidase, translocating H^+ simultaneously through Complexes CIII and CIV (Millar et al. 2011). The other one is a bypass of these two Complexes, where alternative oxidase (AOX) reduces O_2 (Finnegan et al. 2004; Moore et al. 2013). This pathway is also called the cyanide-resistant alternative respiratory pathway, which is genetically expressed by two genes in *Chlamydomonas reinhardtii* (Dinant et al. 2001). Using this pathway, electron flow is uncoupled from ATP synthesis as no membrane potential is developed (Millar et al. 2011). Free energy is won by the electron transport, dispersed as heat, resulting in a smaller yield of respiratory energy (Affourtit et al. 2002; Mathy et al. 2010). In case of highly reduced components of the electron transfer system, AOX eliminates energized electrons, preventing excess production of reactive oxygen species (ROS) (Maxwell et al. 1999). ROS are radicals containing oxygen, such as the hydroxyl radical $^{.}OH$, or oxygen ions, such as singlet oxygen $^1O_2$ or superoxide O_2^-, as well as their reaction products, like hydrogen peroxide H_2O_2 (Auten and Davis 2009). Depending on the context, the function of ROS varies (Lambeth 2007; Auten and Davis 2009).

Furthermore, in the process of photosynthesis ROS are by-products due to the oxidative stress generated by light radiation (Apel and Hirt 2004). Still, light functions as a prerequisite for photosynthesis. The electron transport in chloroplasts is initiated by light energy from H_2O to $NADP^+$ in photosystem II (PS II) to the cytochrome b_6f Complex to photosystem I (PS I) (Stern and Uno 2005). This pathway induces proton translocation from the stroma into the thylakoid lumen in the chloroplast, creating ATP by ATP synthase using transmembrane electrochemical potential (Apel and Hirt 2004; Campbell and Reece 2005). Alternative pathways can be used by electrons that are crucial at fluctuating light intensities, resulting in different requirements of ATP and NADPH (Kramer and Evans 2011). A reorganization of respiratory pathways in mutants of *Chlamydomonas reinhardtii* occurred, such as the activation of CEF, the cyclic electron flow around PS I, an alternative electron flow pathway (AEF) (Cardol et al. 2003; Cardol et al. 2011).

The scientific establishment of the Calvin-Benson cycle, the dark reaction of photosynthesis, and the isolation of chloroplasts without mitochondrial contamination - showing similar rates of CO_2 assimilation as in vivo samples - indicated the independence of chloroplasts from mitochondria (Bassham et al. 1950; Jensen and Bassham 1966). After Mehler discovered the photoreduction of O_2 to H_2O_2 in 1951, Forti and Jagendorf further investigated the Mehler reaction and found that ascorbate enhanced the electron transport from H_2O to O_2, which was coupled to ATP synthesis (Mehler 1951; Forti and Jagendorf 1961). Further findings showed that the Mehler reaction produced the superoxide anion radical O_2^- in PS I at its reducing side, where the oxidization of ascorbate to its free radical (AFR) occurs (Mehler 1951; Miyake and Asada 1992). As AFR acts as an alternative electron acceptor to $NADP^+$, it can ensure the ATP formation rate that is necessary for CO_2 assimilation in the Calvin-Benson cycle (Forti and Ehrenheim 1993; Forti et al. 2006). Thus, O_2 is assumed to be permanently consumed in isolated chloroplasts at steady-state photosynthesis (Egneus et al. 1975). Forti concluded after his experiments in 2008 that mitochondrial respiration initiates photosynthesis, allowing oxidation of electron carriers at stages where the Mehler reaction is inhibited due to lacking O_2 until enough O_2 is produced and the Mehler reaction replaces mitochondrial respiration. Thus, Forti assumed that

chloroplasts functioned autonomously at steady-state photosynthesis due to the Mehler reaction (Forti 2008). More recent findings demonstrate that mitochondria influence the cells on metabolic reactions and on photosynthetic pathways and that a cross-talk between mitochondria and chloroplasts is undeniable (Lemaire et al. 1988; Cardol et al. 2003; Forti 2008), especially when cells are put under stressing conditions. Larosa et al. have shown a crosstalk between mitochondria and chloroplasts by putting mutants of *Chalmydomonas reinhardtii* cells under excess illumination, inducing photo damage and photoinhibition (Larosa et al. 2018).

Photoinhibition

Production of toxic ROS during the light reaction is enhanced when NAD(P)H redox state and ATP turnover are not matched with the activity of the Calvin-Benson cycle (Sharma et al. 2012). Therefore, organisms carrying out photosynthesis are sensitive to environmental fluctuations. The reaction of the organism to the change of abiotic and biotic factors might affect photosynthetic activity to a high extent and, thus, be of bigger relevance than the photosynthetic performance during a steady state (Suorsa et al. 2012; Davis et al. 2016).

Photosynthetic electron transfer reduces oxygen on the acceptor side of photosystem I (PS I), forming superoxide O_2^-, which in turn can further react to H_2O_2, $\cdot OH$ and $^1O_2$ (Mehler 1951; Knox and Dodge 1985; Asada 1999; Zolla and Rinalducci 2002). In case of illumination exceeding photosynthetic capacity, ROS production is enhanced, creating oxidative damage to PS I and PS II, called photoinhibition (Asada 1999; Murata et al. 2007; Sonoike 2011; Sejima et al. 2014; Roach et al. 2015). Already low light intensities are causing damage to PS II (Roach and Krieger-Liszkay 2014), which is why in PS II a repair mechanism has been evolved resynthesizing the subunit D1 of PS II (Pokorska et al. 2009). This repair system ensures photosynthetic electron transfer and cell growth despite elevated light damages. Up to date, no comparable repair mechanism has been discovered yet in PS I, as the whole Complex has to be replaced opposed to PS II, where particularly its subunit D1 is reassembled (Sonoike 1996; MARTIN et al. 1997; Kudoh and Sonoike 2002; Tikkanen and Grebe 2018). Thus, PS II is protecting other components, such

as PS I, from inhibition and damage by reducing the electron transfer rate to PS I, which is subsequently preventing PS I from overexcitation and irreparable consequences (Tiwari et al. 2016). Larosa et al. favor photosynthetic control, a reduction of the electron flux, as a mechanism to protect PS I by decreasing the turnover rate of the cytochrome b_6f Complex under excess radiation and low luminal pH (Finazzi and Rappaport 1998; Tikhonov 2014; Colombo et al. 2016; Larosa et al. 2018). Still, the topic of photoinhibition is a controversial one as there are different known mechanisms that might be involved but have never been confirmed in cells in vivo (Nishiyama et al. 2006).

Photorespiration

The most common definition of algal productivity is photosynthetic efficiency in O_2 production, which can not only be reduced by photoinhibition but also by other mechanisms as such as by the so-called photorespiration. When, instead of CO_2, O_2 is fixed by the enzyme ribulose bisphosphate carbolylase/oxygenase, the toxic by-product 2-phosphoglycolate is produced, which can be detoxified by the photorespiratory reactions to 3-phosphoglycolate. In order to do so, energy intended for photosynthesis is used for photorespiration, resulting in a loss of energy yield and a release of fixed CO_2 (Bauwe et al. 2010).

Light-enhanced dark respiration

The phenomenon of an enhanced O_2 consumption rate after illumination in algal cells is called light-enhanced dark respiration (*LEDR*). According to different references, respiratory substrates accumulated during photosynthetic pathways are assumed to stimulate *LEDR* (Xue et al. 1996; Ekelund 2000; Raghavendra and Padmasree 2003; Mantikci et al. 2017; Sejima et al. 2016). The exact mechanisms of *LEDR* have still remained unknown (Shimakawa et al. 2020). According to Sejma et al. (2016), the O_2 consumption rate after a light period (*LEDR*) corresponds to photorespiration during illumination and is subsequently an indication for the total photosynthesis rate *TP* (net photosynthesis rate *NP* minus photorespiration rate *LEPR*).

The NextGen-O2k

With the new version of the Oxygraph-2k by Oroboros Instruments, the NextGen-O2k (Figure 1), major changes in the firmware had to be done due to the inclusion of the PB-Module, the PhotoBiology-Module, and the Q-Module. Before the development of the NextGen-O2k, following features could be applied using the prior version of the O2k, the FluoRespirometer: O_2 consumption, amperiometric signal, fluorescence signal and potentiometric signal. With the addition of to the PB-Module and the Q-Module, the effect of increasing light intensities on O_2 production (*NP*) in chloroplasts can be measured as well as the redox state of the quinone pool in the mitochchondrial electron transfer system in the NextGen-O2k (Doerrier et al. 2021).

The O2k possesses two separate and independent chambers that consist of Duran glass. Each chamber measures 2 mL of volume that is mixed by magentical stirrers, ensuring a homogeneous solution. Illumination in chambers for control can be used with an LED light from behind the chambers. Experimental temperature is controlled by constant recordings of temperature and Peltier power (Gnaiger 2001). Oxygen flux and concentration is measured by a polarographic oxygen sensor, the POS (Gnaiger and Forstner 1983). Diffusion tight stoppers seal the chambers (Gnaiger 2001).
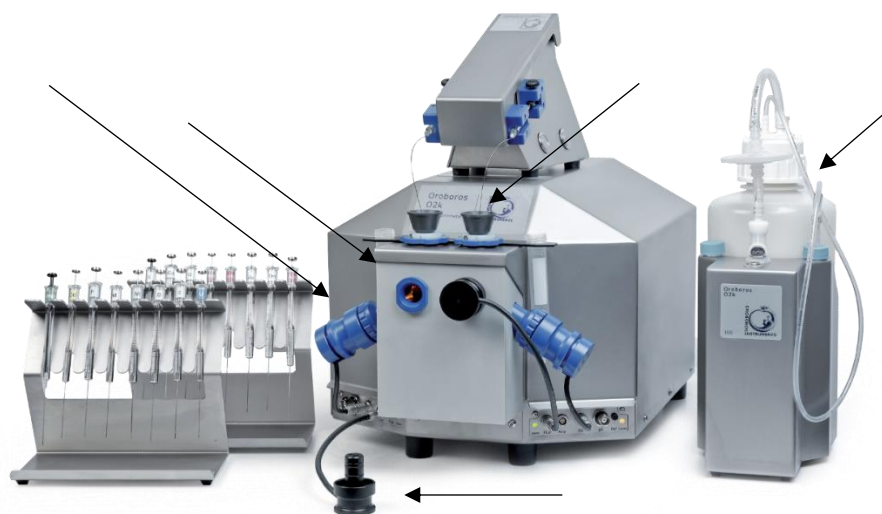

Figure 1: NextGen-O2k illustrated with a PB-sensor, modified after (Doerrier et al. 2018)

PB-Module

The PB-Module was designed based on scientific knowledge of photosynthetic metabolic pathways (Doerrier et al. 2021). Photosynthetic processes are carried out using light in the spectral range between 400 and 700 nm, called photosynthetically active radiation (PAR). Energy conversion occurs most efficiently at wavelengths of blue (400-500 nm) and red (600-700 nm) light (Stern and Uno 2005). Thus, LED lights were included in the PB-sensors emitting PAR in the range of blue and red light. LEDs of white light are available as well as they simulate sun light, i.e. PAR (Campbell and Reece 2005). The PB-Module counts one sensor in each chamber, which need to be attached on the outside of the front chamber window. The light intensities provided by the sensors range from 0 to 5000 µmol photons $m^{-2} s^{-1}$ and can be controlled by using the software by Oroboros Instruments, Datlab 7.4 or higher. Additionally, a photodiode has been implemented in the PB-sensor, which corrects, adjusts and detects the exact light intensity emitted by the LEDs. The effects of different light intensities on the sample, i.e. algal cells, inside of the chambers can be measured by O_2 flux per volume or O_2 flow per cells (Gnaiger 2020; Doerrier et al. 2021).

Materials and methods

Required materials

The required materials and equipment are listed in Table 1.

Table 1: Materials

organisms
Chlamydomonas reinhardtii wt12

chemicals
sodiumbicarbonate
Lugol's solution
Trizma base
NH_4Cl
$MgSO_4 \cdot 7H_2O$
$CaCl_2 \cdot 2H_2O$
K2HPO$_4$
Kropat's trace metals solution

devices and equipment
NextGen-O2k with PB sensors
AlgaeTron AG230 incubator
centrifuge
vortexer
microscope
haemocytometer

Strains and growth conditions

Chlamydomonas reinhardtii wild-type strain *wt12* was kindly provided by Prof. A. Smith, University of Cambridge. The liquid cultures were started in TRIS media, composed of the following chemicals: 2.42 g·L^{-1} Trizma base, 0.38 g·L^{-1} NH_4Cl, 0.1 g·L-1 $MgSO_4 \cdot 7H_2O$, 0.05 g·L^{-1} $CaCl_2 \cdot 2H_2O$, 0.11 g·L^{-1} K_2HPO_4, 0.05 g·L^{-1} KH_2PO_4, 1 mL·L^{-1} Kropat's trace metals solution, adjusted to the pH of 7, then autoclaved and stored at 4 °C (Gorman and Levine 1965; Kropat et al. 2011). TRIS medium was used to autotrophically

grow the culture at 25 °C under 100 µmol·s⁻¹·m⁻² at sterile conditions. The culture flask was kept inside an AlgaeTron AG230 (Photon Systems Instruments) incubator that smoothly agitated the culture and provided a period of 16:8 hours light:dark by a combination of red, green, blue and infrared LEDS. The culture was reduced by 10 mL of culture medium and received 10 mL of fresh TRIS medium three times a week to ensure an exponential growth phase of the algae. Each experiment was conducted one day after a renewal of the medium.
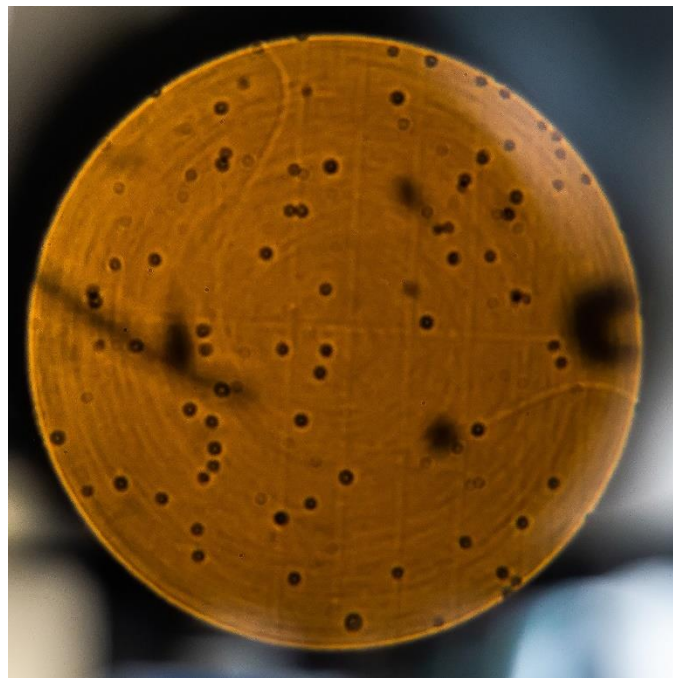
Figure 2: Cells of *Chlamydomonas reinhardtii* under the microscope at a magnification factor of 20

Algae preparation

Before the experimental run, the cell-count concentration $C_{ce,s}$ of the culture was determined. This was performed by the sterile removal of 20 µL of the culture, the dilution of the sample by 20 µL of Lugol's solution and by 160 µL of distilled water afterwards, generating a final dilution of 1:10. The mixture then was vortexed and pipetted onto a haemocytometer (Neubauer chamber, Figure 2). The cell count $N_{ce,s}$, of four fields ($n=4$) per counting grid was performed. Next, the average cell number $\bar{x}$ of the counted

fields was calculated (equation 1) and, subsequently, the cell-count concentration $C_{ce,s}$ by a recalculation of the dilution factor $d=10$ (equation 2).

(1)

$$\bar{x} = \sum_{i=1}^{n=4} \frac{N\text{ce,s}_i}{n}$$

(2)

$$C_{ce,s} = \bar{x} \cdot d \cdot 10\,000$$

With the cell-count concentration $C_{ce,s}$ of the culture, the needed volume $V_{ce,s}$ of the cultural medium could further be quantified by equation 3. V_{G3} equaled the volume of 15 mL needed for the dilution series of the next step. C_{G3} corresponded to the concentration of the highest concentrated dilution group G3 of the dilution series and was aimed for $9 \cdot 10^6$ cells mL^{-1}. The dilution series was consisted of dilution groups G1, G2 and G3. G2 corresponded to 2/3 of G3 and G1 as 1/3 of G3. In total, six cultures ($N=6$) were harvested and diluted with TRIS.

(3)

$$C_{ce,s} \cdot V_{ce,s} = C_{G3} \cdot V_{G3} \rightarrow V_{ce,s} = \frac{C_{G3} \cdot V_{G3}}{C_{ce,s}}$$

While $V_{ce,s}$ was centrifuged for 10 minutes at $1000\,g$ at 25 °C, sodium bicarbonate was added to the microalgal pellet resuspension. Previous internal experiments on *Chlamydomonas reinhardtii* indicated that a concentration of 5 mM of sodium bicarbonate were sufficient to provide a saturation of inorganic carbonate for nutritional purposes at concentrations in the range of this experiment. For this matter a

small mass of sodium bicarbonate was weighed m_{SBC} (for example 14.22 mg), on the basis of which the needed volume of TRIS for a suspension V_{TRIS,CO_2} was calculated, taking the molecular mass of sodium bicarbonate $M_{SBC}=84.01$ mg mmol^{-1} as well as the amount of substance n_{SBC} into account (equation 4 and 5).

(4)

$$n_{SBC} = \frac{m_{SBC}}{M_{SBC}} = \frac{14.22 \text{ mg}}{84.01 \text{ mg mmol}^{-1}} = 0.169 \text{ mmol}$$

(5)

$$V_{TRIS,CO_2} = \frac{n_{SBC}}{C_{SBC}} = \frac{0.169 \text{ mmol}}{5 \text{ mM}} = 0.085 \text{ L} = 85 \text{ mL}$$

V_{TRIS,CO_2} of TRIS was suspended with the weighed mass of sodium bicarbonate m_{SBC} and vortexed. As soon as the centrifugation was finished, the supernatant of the sample of $V_{ce,s}$ was removed and the pellet carefully resuspended by a volume of 15 mL (V_{G3}) of the TRIS-sodium bicarbonate suspension (that measured V_{TRIS,CO_2}), ensuring that any algal cell aggregation was broken.

Next, the dilution series was started by taking 10 mL of V_{G3}, putting it into a new falcon tube and adding 5 mL of the TRIS-sodium bicarbonate suspension (G2). After properly resuspending the second group of the dilution series, 5 mL of V_{G2} was added to another falcon tube which was topped by 5 mL of the TRIS-sodium bicarbonate suspension (G1). After calibrating the O2k, all three dilution groups were added to one O2k each (2.3 mL per chamber), resulting in two technical repeats per O2k.

One 20 µL subsample of each O2k was taken from an O2k chamber prior to closing the chambers and starting the measurements for recounting the cells. This was intended to correct the cell concentrations in the O2k chamber expected from the initial cell count.

Photosynthetic and respiratory measurements

O_2 measurements were performed using the NextGen-O2k. Before every experimental run, the O2k chambers had to be washed three times and air-calibrated at the correct temperature filled with 2.3 mL of the respiration medium used in the following experiment, in this case TRIS at 25 °C at 750 rpm. The correct background had to be loaded in order to minimize any noise by the measuring device. The calibration took up to 1 hour, which is why it had to be done prior to a protocol run. Once the air calibration had finished, the PB-sensors were attached to the O2k, the TRIS medium in the chambers of each O2k was replaced by the dilution series and the stoppers of the chambers were added. Then the protocol SUIT-030 PB ce D070 was started in DatLab, which recorded data points every 2 seconds per chamber. SUIT protocols are intended to examine specific hypotheses in mitochondrial research (Doerrier et al. 2018) and have recently been expanded to photosynthetic approaches (Doerrier et al. 2021).

Between 10 to 20 minutes were necessary to get a stable signal of dark respiration, detected as O_2 flow per cell in amol s^{-1} x^{-1}. After a constant O_2 flow was reached, the PB-sensors were switched on to 10 µmol photons m^{-2} s^{-1} in order to stimulate net photosynthetic O_2 production *NP*. At stepwise increments of light intensity every 3 to 4 minutes, *NP* was stimulated to a maximum of 350 µmol photons m^{-2} s^{-1}, while O_2 concentration increased simultaneously in the chambers. Alternatively, O_2 concentration was prevented from reaching severe hyperoxia by intermittently opening the chambers. The PB-module was shut off after reaching 350 µmol photons m^{-2} s^{-1}, entering another phase of dark respiration until flux stability was attained again. In some protocol runs (Figure 3) the PB-Module was put on again to 350 µmol photons m^{-2} s^{-1} for 10 minutes. Following, data

recording was turned off and the O2k was cleansed. In total, five experimental runs of G1 and G2 were performed, seven of G3.

Data analysis

For data evaluation and graphic visualization DatLab 7.4, Microsoft PowerPoint and Microsoft Excel was used (Table 2).

Table 2: used computer softwares

software	company	purpose
Excel	Microsoft	data recording
DatLab 7.4	Oroboros Instruments	data analysis
PowerPoint	Microsoft	data visualization

After the protocol run, so-called marks were set on the data traces for further data analysis in DatLab. The marks pointed out values for the median of the selected trace area. This was performed for the traces of O_2 flow per cell, volume specific O_2 flux and O_2 concentration.

Moreover, the effect of the light diodes on the O_2 flux while being shut off was examined by running special backgrounds with the intention to reduce background noise (i.e. signal disturbances due to mechanical interferences, not due to actual changes in the O_2 flux). Therefore, the protocol run was performed using the respiration medium TRIS without living sample at varying O_2 levels. This way any fluctuations in the O_2 flux were interpreted as background noise. Additionally, all results were analyzed and compared at data smoothing of 20 dp (data points) and of 5 dp for maximal accuracy of the background.

Results

O₂ flow as a function of the light regime and O₂ concentration

The net O_2 production rate (net photosynthesis *NP*) was stimulated from dark respiration *DR* at normoxia to a maximum by stepwise increments of light intensity (blue light; 10 to 350 $\mu mol \cdot s^{-1} \cdot m^{-2}$). The compensation point at zero *NP*, where respiration and total photosynthesis cancel each other, was reached at a light intensity between 10 and 20 $\mu mol \cdot s^{-1} \cdot m^{-2}$. Light-enhanced dark respiration *LEDR* was detected as a sharp (negative) maximum of respiration immediately after a light period of 60 to 90 minutes (Figure 3). O_2 flow per cell is referred to as I_{O_2} in contrast to O_2 flux per volume abbreviated as J_{O_2}. Whenever the volume-specific O_2 flux or the O_2 flow per cell relate specifically to net photosynthetic O_2 production rate or with light-enhanced photo/dark respiratory O_2 production rate, they are denoted as *NP* or as *LEPR/LEDR*. Each trace depicts two chambers of one O2k, demonstrating the reproducibility of the results outlined in the context of this thesis.
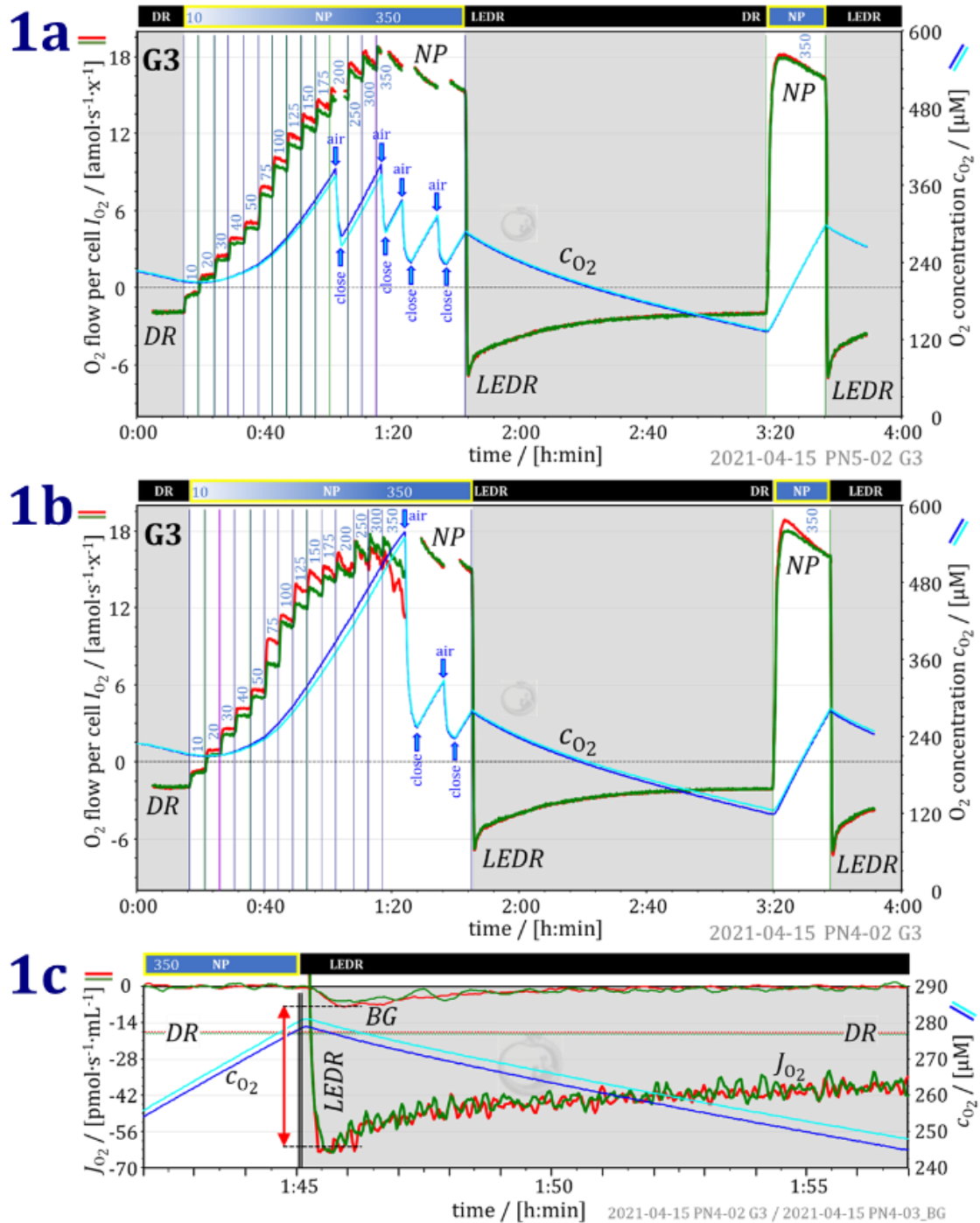
Figure 3: O₂ flow I_{O_2} as a function of the light regime and O₂ concentration c_{O_2}. Superimposed traces of c_{O_2} and I_{O_2} in two O2k-chambers. Maximum net photosynthesis *NP* was obtained at light intensities of 300 to 350 µmol·s⁻¹·m⁻² (vertical numbers). Light-enhanced dark respiration *LEDR* was compared to the instrumental background *BG* (from Went et al. 2021; see Supplement).

Traces displayed in Figures 3a and 3b were recorded simultaneously in two O2k instruments. The four

chambers were filled by subsamples of the same culture stock with identical cell-count concentration.

By intermittently opening the chambers of the O2k, which is illustrated as arrows labelled "air" in the graphic, the O_2 concentration was prevented from reaching severe hyperoxia in the experimental chamber. Opposed to trace 3a, trace 3b shows the increase of O_2 concentrations while the O2k chambers remained closed. O_2 concentration rose to hyperoxic levels due to *NP*. After 12 minutes of illumination at 350 $\mu mol \cdot s^{-1} \cdot m^{-2}$, the O_2 concentration was lowered by intermittently opening the chambers and partial equilibration with air. This restored maximum *NP* (Figure 3b). The following phase of dark respiration showed enhanced respiratory levels compared to the dark respiration phase in the beginning of the protocol.

Figure 3c shows the enlarged peak of *LEDR* of Figure 3c. Additionally, the instrumental background *BG* run has been included in Figure 3c, demonstrating the small transient disturbance of the O_2 signal triggered by the elimination of illumination from 350 to 0 $\mu mol \cdot s^{-1} \cdot m^{-2}$. This disturbance was accounted for in the background correction of the O_2 flux. Thus, the peak measured in the experiment was corrected by the *BG* and assigned to *LEDR*. It was a sharp, (negative) maximum respiratory flux per volume J_{O_2} [$pmol \cdot s^{-1} \cdot mL^{-1}$] at 30 to 60 s after light-dark transitions. *LEDR* returned to *DR* after a dark period of 2 hours. The following rate of *NP* under illumination of 350 $\mu mol \cdot s^{-1} \cdot m^{-2}$ corresponded to the previous maximum *NP*, suggesting no remaining photodamage to the cells.

Dark respiration

In each of the culture harvests, dilution group G3 was diluted 2:3 to G2, which was further diluted 1:2 to G1, such that the concentration of G1 was one third of G3. Cell-count concentration C_{ce} was approximately $9 \cdot 10^6$ $x \cdot mL^{-1}$. A deviation between expected and recounted cell numbers is possible due to cell loss during the harvesting process. The determination of the cell-count concentration seemed to be a trivial task at first. But the recounts (1) did not fit the expected cell concentrations, (2) were much smaller, and (3) were highly variable. This issue of cell counting agrees with the finding of Yépez et al., who investigated respiration normalized for the cell count determined from each experimental chamber in a multi-well instrument. Their results demonstrate that normalization by cell count determined from

the chambers actually increase the coefficient of variation, instead of reducing it (Yépez et al. 2018). This paper was not directly comparable to the approach of this study but demonstrated the general problem of variability of cell counting by using proper statistical analysis. Therefore, the data analysis did not include the recounted cell numbers. Instead, the initial rate of dark respiration DR divided by DR of the corresponding G3 group was utilized for analysis. DR was expressed as O_2 flow per cell [$amol \cdot s^{-1} \cdot x^{-1}$]. In Figure 4, DR of each experimental dilution group was shown relative to DR of G3 of the same culture harvest as were the distributions of the dilution series. DR was, thus, expressed as a dimensionless ratio ([$amol \cdot s^{-1} \cdot x^{-1}$] $\cdot$ [$amol \cdot s^{-1} \cdot x^{-1}$]$^{-1}$) and could be used as a relative cell-count concentration independent of the actual cell count C_{ce}. The values measured by the O2k for DR and maximum NP are listed in Table 3.
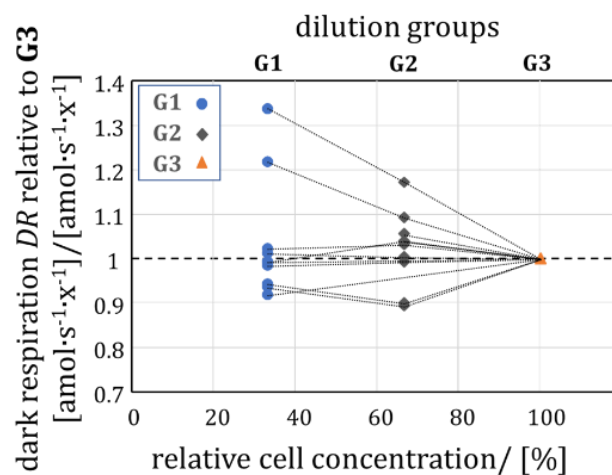

Figure 4: Initial dark respiration DR measured simultaneously in three cell dilutions, expressed relative to dilution group G3 (from Went et al. 2021; see Supplement).

Table 3: O2k measurements: corresponding median of dark respiration *DR,* maximum net photosynthesis *NP* and light-enhanced dark respiration *LEDR* rates [amol·s^{-1}·x^1] at 350 µmol·s^{-1}·m^{-2} of six culture harvests of 3 dilution groups (G1, G2, G3); *LEDR* was evaluated for G3, where the background *BG* could be accounted for

culture harvest	O2k Chamber	G1 [amol·s^1·x^1]		G2 [amol·s^1·x^1]		G3 [amol·s^1·x^1]		
		DR	*NP*	*DR*	*NP*	*DR*	*NP*	*LEDR*
1	A	-2.5854	26.0937	-2.2663	22.2147	-1.9343	18.9502	-9.1157
	B	-2.5844	27.245	-2.3194	22.776	-2.1234	19.6423	-9.2493
2	A	-3.3316	23.605	-3.1777	23.0315	-3.5321	22.6873	-11.9147
	B	-3.4158	25.0109	-3.2623	23.3598	-3.6506	23.0831	
3	A	-2.8664	20.743	-3.0047	21.1242	-2.8893	17.7946	-10.5648
	B	-2.9877	20.5928	-3.0156	21.0675	-3.0372	18.0626	-10.7933
4	A	-5.6063	42.2223	-5.6574	33.8891	-5.4843	28.0006	-20.0785
	B	-5.7482	41.6189	-5.7014	31.0828	-5.6812	28.0164	
5	A			-1.9787	18.7298	-1.9063	16.7943	-6.5047
	B			-2.0365	19.1312	-1.9324	16.9815	-5.8595
6	A	-1.8163	20.125			-1.9786	16.1993	-6.7969
	B	-1.8891	20.6931			-1.9043	17.1997	-6.6847
	A					-1.8633	18.4034	-6.8141
	B					-1.8877	17.9764	-9.1157

In order to provide further clarification, two assumptions had to be considered: (1) the cell count within each dilution group might vary from day to day due to incorrect cell-counting and (2) the cells might have different photosynthetic activity from day to day. Thus, a different way for the comparison of the results had to be used. Setting G3 as equivalent to 100 % of the cell count within each dilution series, the rates of *DR* of G1 and G2 were divided by *DR* of G3 at 100 %. No correlation between *DR*, expressed relative to *DR* of G3, and the relative cell-count concentration of each dilution group was found (Figure 4). The independence of *DR* of dilution provided the basis for normalizing *NP* and *LEDR* for *DR* in each dilution group, allowing for comparison of all experiments independent of day-to-day variability in the cell count. In summary, maximum *NP* was uniformly O_2 dependent at all dilutions (Figure 6.)

Maximum net photosynthesis as a function of cell concentration and O_2 concentration

A stepwise increase of light intensity stimulated net photosynthesis *NP* to a maximum, while O_2 concentration rose from 220 µM to 400 µM (G1), 520 µM (G2) and 550 µM (G3), depending on the cell-

count per volume in the closed reaction chamber (Figure 5). At higher cell concentration (G3), the *NP* capacity was reduced compared to *NP* at lower cell concentration (G1). Therefore, experiments at lower cell-count concentrations resulted in higher *NP* rates at maximum illumination linked to a lower O_2 concentration. Conversely, traces at higher cell-count concentrations showed the opposite relation – lower *NP* rates at higher O_2 concentrations. This correlation has been further illustrated in Figure 6.
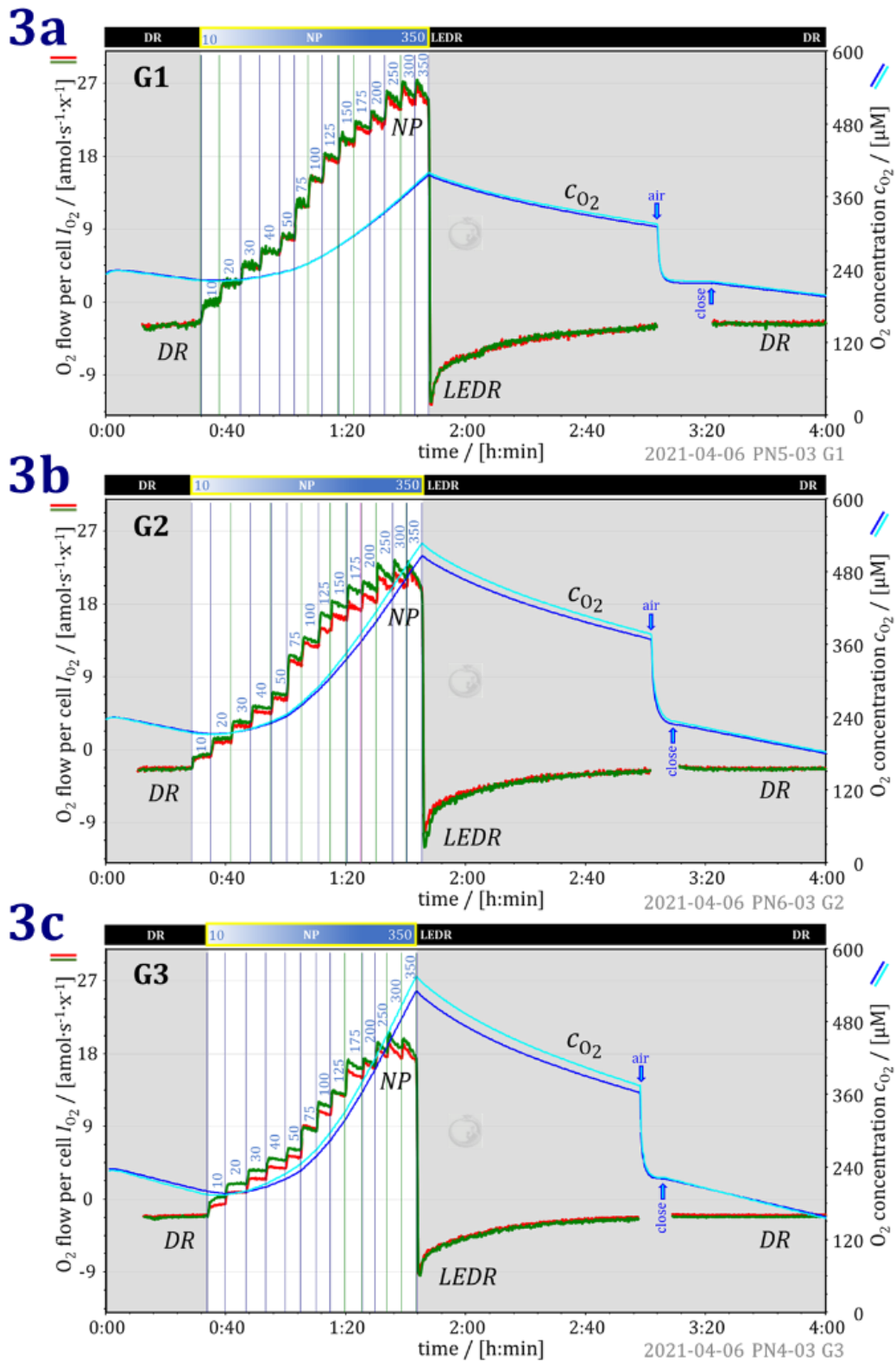
Figure 5: O₂ flow at different cell concentrations (G1 to G3) determines O₂ concentrations at increasing light intensities in the closed chamber. Superimposed traces of oxygen concentration c_{O_2} and O₂ flow per cell I_{O_2} in two O2k-chambers. Maximum net photosynthesis *NP* was obtained at light intensities of 300 to 350 µmol·s⁻¹·m⁻² (vertical numbers). *DR* returned to initial levels 2 hours after the *LEDR* peak (from Went et al. 2021; see Supplement).

Oxygen dependence of net photosynthesis and light-enhanced dark respiration

O_2 fluxes were expressed relative to dark respiration measured in the beginning of the experiment *DR* (see Figure 4 and Table 4). This normalization yields flux control ratios entirely independent of cell counts (Gnaiger 2020). Independent of dilution, *NP* was inhibited gradually from normoxia to severe hyperoxia by up to 40 %, as illustrated in figure 6. No differences could be identified comparing measurements taken in the morning (am) or in the afternoon (pm). Rates of light-enhanced dark respiration *LEDR* measured at normoxia and hyperoxia were 3- to 4-fold higher than the initial rate of *DR*, shown with G3. *LEDR* did not significantly depend on O_2 concentration (Figure 4). Any possible bias due to instrumental background corrections are minimized at G3 with the highest cell-count concentration, where volume-specific fluxes are higher than in experiments with G1 and G2. Therefore, Figure 6 emphasizes the results with G3. The values used for the O_2 fluxes relative to DR (Table 4) were taken from Table 3, whereas the O2k measurements of the corresponding O_2 concentrations from Table 4.
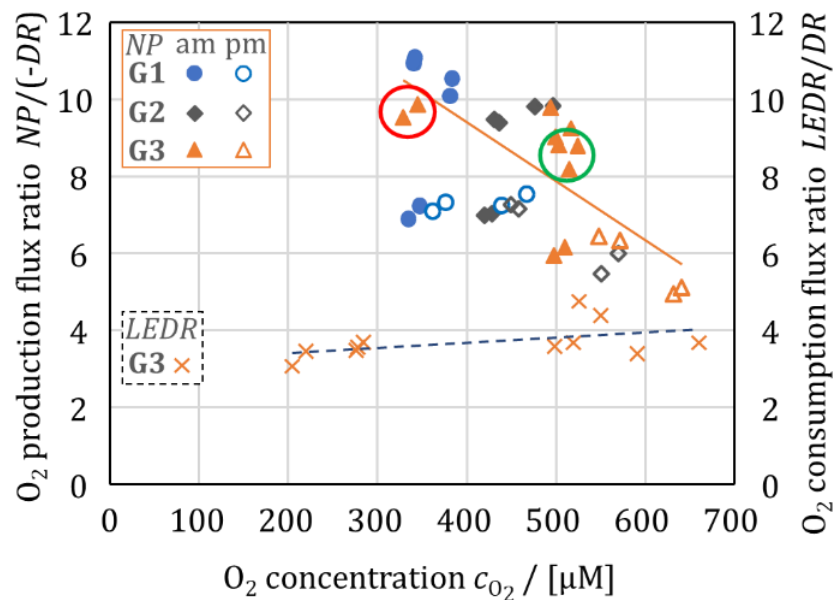

Figure 6: Oxygen dependence of net photosynthesis *NP* and light-enhanced dark respiration *LEDR*. O_2 flux ratios normalized for dark respiration *DR*. Red and green circles: data from Figures 3a and 3b (from Went et al. 2021; see Supplement).

Table 4: O2k measurements: median of O_2 production rates (*NP* or *LEDR*) relative to *DR* with the corresponding median of oxygen concentration c_{O2} at different dilution steps (G1, G2, G3) of all harvest cultures (*N*=6). *LEDR* was analyzed for G3 and was reduced by the background correction *BG*

harvest culture	O2k chamber	G1		G2		G3			
		<u>NP</u> DR	c_{O2} in µM	<u>NP</u> DR	c_{O2} in µM	<u>NP</u> DR	c_{O2} in µM	<u>LEDR-BG</u> DR	c_{O2} in µM
1	A	10.09	381.06	9.80	476.66	9.80	493.89	0.94	525.79
	B	10.54	383.65	9.82	496.86	9.25	516.14	0.94	549.68
2	A	7.09	362.23	7.25	449.93	6.42	548.41	0.93	591.27
	B	7.32	376.78	7.16	458.27	6.32	571.89		
3	A	7.24	347.27	7.03	428.44	6.16	509.79	0.98	519.37
	B	6.89	334.67	6.99	420.20	5.95	497.19	1.00	498.07
4	A	7.53	467.38	5.99	570.56	5.11	640.74	0.97	659.66
	B	7.24	439.76	5.45	551.52	4.93	631.46		
5	A			9.47	430.94	8.81	503.12	2.29	219.70
	B			9.39	436.35	8.79	524.33	2.57	204.17
6	A	11.08	341.90			8.19	514.53	1.86	276.10
	B	10.95	340.58			9.03	499.11	1.79	278.31
	A					9.88	344.40	1.21	284.04
	B					9.52	328.21		

Discussion

Oxygen dependence of net photosynthesis and its potential cause of photoinhibition

Photoinhibition is a process coupled to photosynthesis that still has not been fully resolved (Shimakawa et al. 2020). Its impact - especially with involvement of ROS - on photosynthetic yield is well established but its origin is a controversial topic (Nishiyama et al. 2006). In order to understand the process, reproducible and reliable data is required (Baker 2016). Reproducibility was ensured with the NextGen-O2k by accurate calibrations and detailed background corrections to account for disturbances of the signal. These include O_2 diffusion into or out of the closed chamber and the side effect of the illumination regime, which is neglected by other conventionally applied instruments (Shimakawa et al. 2020). The unique resolution of O_2 concentration and O_2 flux, measured in the O2k, generated highly accurate real-time estimations of photosynthesis, apparent from the replicates in the two independent chambers.

The results clearly show that photoinhibition already started at low light intensities around 75 $\mu mol \cdot s^{-1} \cdot m^{-2}$ (Figure 3). Photoinhibition has been identified as an inevitable side effect of photosynthesis at any light intensity (Gombos et al. 1994; Tyystjärvi and Aro 1996; Anderson and Chow 2002). The effect of photoinhibition increased at higher light intensities. Surprisingly, equally concentrated cell cultures reached different levels of maximum O_2 production at the same light intensity, depending on the prevailing O_2 concentration in the reaction chamber (Figure 3). This indicated that photoinhibition was directly linked to high O_2 concentration. With increasing O_2 concentration photoinhibition became more pronounced (Figure 6). This agrees with the fact that high light intensity and high O_2 concentration - the product of photosynthetic activity – are a critical and frequently predominant combination, which results in damage of the photosynthetic apparatus (Hall 2017). Of course, O_2 production rises with increasing levels of illumination due to higher rates of photosynthesis in closed and diffusion-limited systems. As it is known that high O_2 levels stimulate ROS production (see Chapters 1.2 and 1.3), this indicates that the inhibition at high O_2 concentration was linked to ROS-induced oxidative stress (Asada 1999; Murata et al. 2007; Sonoike 2011; Sejima et al. 2014; Roach et al. 2015). ROS in turn block repair mechanisms that protect against photodamage (Nishiyama et al. 2001; Nishiyama et al. 2004; Jimbo et al. 2013). The mechanisms of photoinhibition due to hyperoxia are beyond the scope of the present study.

After a dark period of 2 hours, *LEDR* returned to the initial rate of *DR*. Moreover, *NP* recovered and reached the same levels of O_2 flow at a second period of maximum illumination at 350 $\mu mol \cdot s^{-1} \cdot m^{-2}$ after this period of *DR*. Thus, the effects of hyperoxia and photoinhibition showed no remaining damage to the cells, which suggests that O_2-dependent inhibition damage was restricted to PS II (Kudoh and Sonoike 2002).

CO_2 was available at saturating concentrations during all experiments, which is known to trigger the Mehler reaction leading to H_2O_2 production (Roach et al. 2015). Recently, Neofotis et al. (2021) showed ROS accumulation as a response to hyperoxia in wild type strain CC-1009 of *Chlamydomonas reinhardtii*. After hyperoxic exposure of 6 to 31 hours, H_2O_2 concentration increased 3-fold (Neofotis et al. 2021).

Nishiyama et al. (2006) suggest that photodamage is purely dependent on light, which was not supported by the findings in Figure 3. The O_2-evolving Complex is impaired by light (Nishiyama et al. 2006). These authors could not identify the mechanisms causing the impairment of the O_2-evolving Complex. However, the results obtained in this thesis might provide an explanation for this phenomenon. As this Complex is directly involved in O_2 production during photosynthesis, it follows that O_2 may inhibit the O_2-evolving Complex by substrate inhibition. Taken together, the apparent controversy of the different results may be resolved by emphasizing the synergy of ROS-dependent and ROS-independent effects of photoinhibition, both induced by high O_2 concentrations.

Oxygen independence of light-enhanced dark respiration

In Figure 6, a significant correlation of light-enhanced dark respiration and O_2 concentration was not indicated. Thus, if *LEDR* actually was an equivalent to light-enhanced photorespiration *LEPR* (Xue et al. 1996; Sejima et al. 2016), then its inhibitory effect on net photosynthesis would not be significantly O_2-dependent either. These observations, (1) the decline of *NP* as a function of O_2 concentration and (2) the O_2 independence of *LEDR* indicate a primary inhibition of total photosynthesis *TP* at high O_2 concentrations, which is photoinhibition. Therefore, the primary cause for reduction of net photosynthesis is not a stimulation of photorespiration but O_2 dependent photoinhibition.

The mechanism causing a 3- to 4-fold increase of *LEDR* compared to *DR* was not the subject of this thesis. In any case, these findings prove the importance of the crosstalk between mitochondria and chloroplasts. Consequently, a better understanding of chloroplast and mitochondrial bioenergetics is crucial in order to understand the efficiency of photosynthesis and, thus, to help maximize the outcome of algal exploitations.

Maximum net photosynthesis as a function of cell concentration and O_2 concentration

A common assumption that cell shading could have a negative influence on photosynthetic activity at higher cell-count concentrations (G3) could be excluded by comparing Figures 3 and 5. In Figure 5, G3 reached a lower rate of *NP* compared to G1. But Figure 3 clearly showed that the diminished *NP* rate was a consequence of hyperoxic inhibition of photosynthesis - not a consequence of cell shading. The concept of cell shading would be invoked in the absence of an effect of O_2 concentration on *NP*. Thus, measurement of O_2 dependence of *NP* in different dilution groups (G1, G2, G3) was decisive for separating the effects of shading and O_2 kinetics (Figure 5). As higher cell-count concentrations resulted in higher O_2 concentrations, higher *NP* rates correlated with lower cell counts. However, this was not a causative correlation since maximum *NP* was shown to be indirectly linked to cell-count concentration. The actual mechanism explaining that more cells resulted in lower *NP* rates in a closed system was the higher O_2 production leading to inhibitory O_2 concentrations.

A limitation in the present study relates to the lack of quality-controlled cell counting. More precise methods for determination of cell-count concentrations will support reproducibility and strengthen the conclusions.

Conclusions and future perspectives

The results of this thesis contribute to the understanding of the relation between mitochondria and chloroplasts by analyzing inhibitory effects of high O_2 concentrations on photosynthesis and thus emphasizing the importance of regulating O_2 levels in biotechnology. Opposed to expectations, the decline of net O_2 production under hyperoxia was not caused by compensatory light-enhanced photorespiration *LEPR*, if light-enhanced dark respiration *LEDR* is proportional to *LEPR* (Xue et al. 1996; Shimakawa et al. 2020), but by inhibition of photosynthesis at high O_2 concentrations. *LEDR* was 3- to 4-fold higher than steady-state dark respiration *DR*. *DR* returned to initial levels 2 hours after the *LEDR*

peak. It will be interesting to investigate the mechanisms involved during that phase as it might be connected to the repair mechanisms of photodamage, which were inhibited during illumination due to hyperoxia.

The simultaneous protocol run at identical cell-count concentrations and different O_2 levels allowed to demonstrate the significance of O_2 as an inhibitory factor of photosynthesis. The results have shown photoinhibition by rising O_2 concentrations. In relevant scientific literature controversial findings have been reported in the context of photoinhibition. Noticeably, O_2 dependence is a topic that has received little attention and its importance has been largely neglected. ROS production due to high O_2 might be one effect but also other mechanisms and reactions might exert an influence on chloroplasts. The NextGen-O2k provides the possibility to measure O_2 concentrations, O_2 production and consumption rates as well as ROS production simultaneously. Thus, further investigations on the connection between O_2 concentration and ROS production are of highest interest to understand the inhibitory effect of O_2 on photosynthesis.

Further approaches relevant to the topic of this study will provide further clarifications on the crosstalk of mitochondria and chloroplasts. The time span of excess light should be extended in order to induce further photoinhibition. Irreversible damage to the cells might occur in a bigger time frame. Mechanisms involved in PS I might be provoked and investigated because irreversible damage is ascribed to reactions in PS I, where repair mechanisms have not been fully investigated yet (Larosa et al. 2018). The concentration of inorganic carbon should be changed as well as abundant carbon triggers the Mehler reaction, which further triggers ROS production (Roach et al. 2015). These investigations will support translation of research into process optimization and biotechnological applications. Improved algal exploitation is required as a contribution to sustainable food and fuel production, supporting environmental protection and addressing current challenges of climate change.

Publication bibliography

Affourtit, C.; Albury, M. S.; Crichton, P. G.; Moore, A. L. (2002): Exploring the molecular nature of alternative oxidase regulation and catalysis. In *FEBS Letters* 510 (3), pp. 121–126. DOI: 10.1016/S0014-5793(01)03261-6.

Anderson, J. M.; Chow, W. S. (2002): Structural and functional dynamics of plant photosystem II. In *Philosophical transactions of the Royal Society of London. Series B, Biological sciences* 357 (1426), 1421-30; discussion 1469-70. DOI: 10.1098/rstb.2002.1138.

Apel, K.; Hirt, H. (2004): Reactive oxygen species: metabolism, oxidative stress, and signal transduction. In *Annual Review of Plant Biology* 55 (1), pp. 373–399. DOI: 10.1146/annurev.arplant.55.031903.141701.

Asada, K. (1999): THE WATER-WATER CYCLE IN CHLOROPLASTS: Scavenging of Active Oxygens and Dissipation of Excess Photons. In *Annual review of plant physiology and plant molecular biology* 50 (1), pp. 601–639. DOI: 10.1146/annurev.arplant.50.1.601.

Auten, R. L.; Davis, J. M. (2009): Oxygen toxicity and reactive oxygen species: the devil is in the details. In *Pediatr Res* 66 (2), pp. 121–127. DOI: 10.1203/PDR.0b013e3181a9eafb.

Baker, M. (2016): 1,500 scientists lift the lid on reproducibility. In *Nature* 533 (7604), pp. 452–454. DOI: 10.1038/533452a.

Bassham, J. A.; Benson, A. A.; Calvin, M. (1950): The path of carbon in photosynthesis. In *The Journal of biological chemistry* 185 (2), pp. 781–787. Available online at https://pubmed.ncbi.nlm.nih.gov/14774424/.

Bauwe, H.; Hagemann, M.; Fernie, A. R. (2010): Photorespiration: players, partners and origin. In *Trends in Plant Science* 15 (6), pp. 330–336. DOI: 10.1016/j.tplants.2010.03.006.

Campbell, N. A.; Reece, J. B. (2005): *Campbell biology*. Boston: Benjamin Cummings / Pearson

Cardol, P.; Forti, G.; Finazzi, G. (2011): Regulation of electron transport in microalgae. In *Biochimica et biophysica acta* 1807 (8), pp. 912–918. DOI: 10.1016/j.bbabio.2010.12.004.

Cardol, P.; Gloire, G.; Havaux, M.; Remacle, C.; Matagne, R.; Franck, F. (2003): Photosynthesis and state transitions in mitochondrial mutants of *Chlamydomonas reinhardtii* affected in respiration. In *Plant Physiology* 133 (4), pp. 2010–2020. DOI: 10.1104/pp.103.028076.

Colombo, M.; Suorsa, M.; Rossi, F.; Ferrari, R.; Tadini, L.; Barbato, R.; Pesaresi, P. (2016): Photosynthesis Control: An underrated short-term regulatory mechanism essential for plant viability. In *Plant Signaling & Behavior* 11 (4), e1165382. DOI: 10.1080/15592324.2016.1165382.

Davis, G. A.; Kanazawa, A.; Schöttler, M. A.; Kohzuma, K.; Froehlich, J. E.; Rutherford, A. W. et al. (2016): Limitations to photosynthesis by proton motive force-induced photosystem II photodamage. In *eLife* 5. DOI: 10.7554/eLife.16921.

Dinant, M.; Baurain, D.; Coosemans, N.; Joris, B.; Matagne, R. F. (2001): Characterization of two genes encoding the mitochondrial alternative oxidase in *Chlamydomonas reinhardtii*. In *Curr Genet* 39 (2), pp. 101–108. DOI: 10.1007/s002940000183.

Doerrier, C.; Daltro Cardoso, L.; Huete-Ortega, M.; Komlodi, T. (2021): Deliverable 2.0. Scientific report for each module of the NextGen-O2k. Next Generation Instrument for In-Depth Analysis of Mitochondrial Fitness. Oroboros Instruments, European Union.

Doerrier, C.; Garcia-Souza, L. F.; Krumschnabel, G.; Wohlfarter, Y.; Mészáros, A. T.; Gnaiger, E. (2018): High-Resolution FluoRespirometry and OXPHOS Protocols for Human Cells, Permeabilized Fibers from Small Biopsies of Muscle, and Isolated Mitochondria. In António J. M. Moreno, Carlos M. Palmeira (Eds.): Mitochondrial bioenergetics. Methods and protocols, vol. 1782. Second edition. New York: Humana Press (Springer protocols, 1782), pp. 31–70.

Egneus, H.; Heber, U.; Matthiesen, U.; Kirk, M. (1975): Reduction of oxygen by the electron transport chain of chloroplasts during assimilation of carbon dioxide. In *Biochimica et Biophysica Acta (BBA) - Bioenergetics* 408 (3), pp. 252–268. DOI: 10.1016/0005-2728(75)90128-0.

Ekelund, N. G. A. (2000): Interactions between photosynthesis and 'light-enhanced dark respiration' (LEDR) in the flagellate *Euglena gracilis* after irradiation with ultraviolet radiation. In *Journal of Photochemistry and Photobiology B: Biology* 55 (1), pp. 63–69. DOI: 10.1016/S1011-1344(00)00029-4.

Finazzi, G.; Rappaport, F. (1998): In vivo characterization of the electrochemical proton gradient generated in darkness in green algae and its kinetic effects on cytochrome b6f turnover. In *Biochemistry* 37 (28), pp. 9999–10005. DOI: 10.1021/BI980320J.

Finnegan, P. M.; Soole, K. L.; Umbach, A. L. (2004): Alternative mitochondrial electron transport proteins in higher plants, p. 163.

Forti, G. (2008): The role of respiration in the activation of photosynthesis upon illumination of dark adapted *Chlamydomonas reinhardtii*. In *Biochimica et biophysica acta* 1777 (11), pp. 1449–1454. DOI: 10.1016/j.bbabio.2008.08.011.

Forti, G.; Agostiano, A.; Barbato, R.; Bassi, R.; Brugnoli, E.; Finazzi, G. et al. (2006): Photosynthesis research in Italy: a review. In *Photosynthesis Research* 88 (3), pp. 211–240. DOI: 10.1007/s11120-006-9054-z.

Forti, G.; Ehrenheim, A. M. (1993): The role of ascorbic acid in photosynthetic electron transport. In *Biochimica et Biophysica Acta (BBA) - Bioenergetics* 1183 (2), pp. 408–412. DOI: 10.1016/0005-2728(93)90246-C.

Forti, G.; Jagendorf, A. T. (1961): Photosynthetic phosphorylation in the absence of redox dyes: Oxygen and ascorbate effects. In *Biochimica et biophysica acta* 54 (2), pp. 322–330. DOI: 10.1016/0006-3002(61)90372-9.

Gnaiger, E. (2001): Bioenergetics at low oxygen: dependence of respiration and phosphorylation on oxygen and adenosine diphosphate supply. Respir Physiol 128:277-97.

Gnaiger, E. (2020): Mitochondrial pathways and respiratory control. An introduction to OXPHOS analysis. 5th ed. Bioenerg Commun 2020.2: 112 pp. doi:10.26124/bec:2020-0002

Gnaiger, E.; Forstner, H. (1983): Polarographic Oxygen Sensors. Aquatic and Physiological Applications. Berlin, Heidelberg: Springer Berlin Heidelberg.

Gombos, Z.; Wada, H.; Murata, N. (1994): The recovery of photosynthesis from low-temperature photoinhibition is accelerated by the unsaturation of membrane lipids: a mechanism of chilling tolerance. In *Proceedings of the National Academy of Sciences of the United States of America* 91 (19), pp. 8787–8791. DOI: 10.1073/pnas.91.19.8787.

Gorman, D. S.; Levine, R. P. (1965): Cytochrome f and plastocyanin: their sequence in the photosynthetic electron transport chain of *Chlamydomonas reinhardi*. In *Proceedings of the National Academy of Sciences of the United States of America* 54 (6), pp. 1665–1669. DOI: 10.1073/pnas.54.6.1665.

Hall, C. Collin (2017): Photosynthesis and Hyperoxia. Disseration Thesis for Doctor of Philosophy. 10277824 volumes: ProQuest Dissertations Publishing. Available online at https://search.proquest.com/openview/74527c811b956b9560b8b3a472587cfd/1?pq-origsite=gscholar&cbl=18750&diss=y.

Harris, E. H. (2001): *CHLAMYDOMONAS* AS A MODEL ORGANISM. In *Annual review of plant physiology and plant molecular biology* 52 (1), pp. 363–406. DOI: 10.1146/annurev.arplant.52.1.363.

Jensen, R. G.; Bassham, J. A. (1966): Photosynthesis by isolated chloroplasts. In *Proceedings of the National Academy of Sciences of the United States of America* 56 (4), pp. 1095–1101. DOI: 10.1073/pnas.56.4.1095.

Jimbo, H.; Noda, A.; Hayashi, H.; Nagano, T.; Yumoto, I.; Orikasa, Y. et al. (2013): Expression of a highly active catalase VktA in the cyanobacterium *Synechococcus elongatus* PCC 7942 alleviates the photoinhibition of photosystem II. In *Photosynth Res* 117 (1-3), pp. 509–515. DOI: 10.1007/s11120-013-9804-7.

Knox, J. P.; Dodge, A. D. (1985): Singlet oxygen and plants. In *Phytochemistry* 24 (5), pp. 889–896. DOI: 10.1016/S0031-9422(00)83147-7.

Kramer, D. M.; Evans, J. R. (2011): The importance of energy balance in improving photosynthetic productivity. In *Plant Physiology* 155 (1), pp. 70–78. DOI: 10.1104/pp.110.166652.

Kropat, J.; Hong-Hermesdorf, A.; Casero, D.; Ent, P.; Castruita, M.; Pellegrini, M. et al. (2011): A revised mineral nutrient supplement increases biomass and growth rate in *Chlamydomonas reinhardtii*. In *The Plant Journal* 66 (5), pp. 770–780. DOI: 10.1111/j.1365-313X.2011.04537.x.

Kudoh, H.; Sonoike, K. (2002): Irreversible damage to photosystem I by chilling in the light: cause of the degradation of chlorophyll after returning to normal growth temperature. In *Planta* 215 (4), pp. 541–548. DOI: 10.1007/s00425-002-0790-9.

Lambeth, J. D. (2007): Nox enzymes, ROS, and chronic disease: an example of antagonistic pleiotropy. In *Free Radical Biology and Medicine* 43 (3), pp. 332–347. DOI: 10.1016/j.freeradbiomed.2007.03.027.

Larosa, V.; Meneghesso, A.; La Rocca, N.; Steinbeck, J.; Hippler, M.; Szabò, I.; Morosinotto, T. (2018): Mitochondria Affect Photosynthetic Electron Transport and Photosensitivity in a Green Alga. In *Plant Physiology* 176 (3), pp. 2305–2314. DOI: 10.1104/pp.17.01249.

Lemaire, C.; Wollman, F. A.; Bennoun, P. (1988): Restoration of phototrophic growth in a mutant of *Chlamydomonas reinhardtii* in which the chloroplast atpB gene of the ATP synthase has a deletion: an example of mitochondria-dependent photosynthesis. In *Proceedings of the National Academy of Sciences of the United States of America* 85 (5), pp. 1344–1348. DOI: 10.1073/pnas.85.5.1344.

Mantikci, M.; Hansen, J. L.S.; Markager, S. (2017): Photosynthesis enhanced dark respiration in three marine phytoplankton species. In *Journal of Experimental Marine Biology and Ecology* 497, pp. 188–196. DOI: 10.1016/j.jembe.2017.09.015.

Martin, R. E.; Thomas, D. J.; Tucker, D. E.; Herbert, S. K. (1997): The effects of photooxidative stress on photosystem I measured in vivo in *Chlamydomonas*. In *Plant Cell Environ* 20 (12), pp. 1451–1461. DOI: 10.1046/J.1365-3040.1997.D01-47.X.

Mathy, G.; Cardol, P.; Dinant, M.; Blomme, A.; Gérin, S.; Cloes, M. et al. (2010): Proteomic and functional characterization of a *Chlamydomonas reinhardtii* mutant lacking the mitochondrial alternative oxidase 1. In *Journal of Proteome Research* 9 (6), pp. 2825–2838. DOI: 10.1021/pr900866e.

Maxwell, D. P.; Wang, Y.; McIntosh, L. (1999): The alternative oxidase lowers mitochondrial reactive oxygen production in plant cells. In *Proceedings of the National Academy of Sciences of the United States of America* 96 (14), pp. 8271–8276. DOI: 10.1073/pnas.96.14.8271.

Mehler, A. H. (1951): Studies on reactions of illuminated chloroplasts. In *Archives of Biochemistry and Biophysics* 33 (1), pp. 65–77. DOI: 10.1016/0003-9861(51)90082-3.

Melis, A. (2007): Photosynthetic H_2 metabolism in *Chlamydomonas reinhardtii* (unicellular green algae). In *Planta* 226 (5), pp. 1075–1086. DOI: 10.1007/s00425-007-0609-9.

Millar, A. H.; Whelan, J.; Soole, K. L.; Day, D. A. (2011): Organization and regulation of mitochondrial respiration in plants. In *Annual Review of Plant Biology* 62, pp. 79–104. DOI: 10.1146/annurev-arplant-042110-103857.

Miyake, C.; Asada, K (1992): Thylakoid bound ascorbate peroxidase in spinach chloroplasts and photoreduction of its primary oxidation product monodehydroascorbate radicals in thylakoids. In *Plant Cell Physiol* 33, p. 541.

Moore, Anthony L.; Shiba, Tomoo; Young, Luke; Harada, Shigeharu; Kita, Kiyoshi; Ito, Kikukatsu (2013): Unraveling the heater: new insights into the structure of the alternative oxidase. In *Annual Review of Plant Biology* 64 (1), pp. 637–663. DOI: 10.1146/annurev-arplant-042811-105432.

Murata, N.; Takahashi, S.; Nishiyama, Y.; Allakhverdiev, S. I. (2007): Photoinhibition of photosystem II under environmental stress. In *Biochimica et biophysica acta* 1767 (6), pp. 414–421. DOI: 10.1016/j.bbabio.2006.11.019.

Nagy, V.; Podmaniczki, A.; Vidal-Meireles, A.; Tengölics, R.; Kovács, L.; Rákhely, G. et al. (2018): Water-splitting-based, sustainable and efficient H_2 production in green algae as achieved by substrate

limitation of the Calvin-Benson-Bassham cycle. In *Biotechnol Biofuels* 11 (1), p. 69. DOI: 10.1186/s13068-018-1069-0.

Neofotis, P.; Temple, J.; Tessmer, O. L.; Bibik, J.; Norris, N.; Poliner, E. et al. (2021): The Induction of Pyrenoid Synthesis by Hyperoxia and its Implications for the Natural Diversity of Photosynthetic Responses in *Chlamydomonas*. In *bioRxiv*, 2021.03.10.434646. DOI: 10.1101/2021.03.10.434646.

Nishiyama, Y.; Yamamoto, H.; Allakhverdiev, S. I.; Inaba, M.; Yokota, A.; Murata, N. (2001): Oxidative stress inhibits the repair of photodamage to the photosynthetic machinery. In *The EMBO Journal* 20 (20), pp. 5587–5594. DOI: 10.1093/emboj/20.20.5587.

Nishiyama, Yoshitaka; Allakhverdiev, S. I.; Murata, N. (2006): A new paradigm for the action of reactive oxygen species in the photoinhibition of photosystem II. In *Biochimica et biophysica acta* 1757 (7), pp. 742–749. DOI: 10.1016/j.bbabio.2006.05.013.

Nishiyama, Y.; Allakhverdiev, S. I.; Yamamoto, Hiroshi; Hayashi, Hidenori; Murata, Norio (2004): Singlet oxygen inhibits the repair of photosystem II by suppressing the translation elongation of the D1 protein in *Synechocystis sp*. PCC 6803. In *Biochemistry* 43 (35), pp. 11321–11330. DOI: 10.1021/bi036178q.

Pokorska, B.; Zienkiewicz, M.; Powikrowska, M.; Drozak, A.; Romanowska, E. (2009): Differential turnover of the photosystem II reaction centre D1 protein in mesophyll and bundle sheath chloroplasts of maize. In *Biochimica et biophysica acta* 1787 (10), pp. 1161–1169. DOI: 10.1016/j.bbabio.2009.05.002.

Raghavendra, A. S.; Padmasree, K. (2003): Beneficial interactions of mitochondrial metabolism with photosynthetic carbon assimilation. In *Trends in Plant Science* 8 (11), pp. 546–553. DOI: 10.1016/J.TPLANTS.2003.09.015.

Roach, T.; Krieger-Liszkay, A. (2014): Regulation of photosynthetic electron transport and photoinhibition. In *Current Protein & Peptide Science* 15 (4), pp. 351–362. DOI: 10.2174/1389203715666140327105143.

Roach, T.; Na, C. S.; Krieger-Liszkay, A. (2015): High light-induced hydrogen peroxide production in *Chlamydomonas reinhardtii* is increased by high CO_2 availability. In *The Plant Journal* 81 (5), pp. 759–766. DOI: 10.1111/tpj.12768.

Rochaix, J. D. (1995): *Chlamydomonas reinhardtii* as the photosynthetic yeast. In *Annual review of genetics* 29, pp. 209–230. DOI: 10.1146/annurev.ge.29.120195.001233.

Rochaix, J.-D. (2014): *Chlamydomonas reinhardtii.* In Sydney Brenner, Jeffrey H. Miller (Eds.): Brenner's Encyclopedia of Genetics. 2nd ed. Saint Louis: Elsevier Science, pp. 521–524. Available online at https://www.sciencedirect.com/science/article/pii/B9780123749840002308.

Scoma, A.; Durante, L.; Bertin, L.; Fava, F. (2014): Acclimation to hypoxia in *Chlamydomonas reinhardtii*: can biophotolysis be the major trigger for long-term H_2 production? In *New Phytologist* 204 (4), pp. 890–900. DOI: 10.1111/nph.12964.

Sejima, T.; Hanawa, H.; Shimakawa, G.; Takagi, D.; Suzuki, Y.; Fukayama, H. et al. (2016): Post-illumination transient O_2-uptake is driven by photorespiration in tobacco leaves. In *Physiol Plantarum* 156 (2), pp. 227–238. DOI: 10.1111/ppl.12388.

Sejima, T.; Takagi, D.; Fukayama, H.; Makino, A.; Miyake, C. (2014): Repetitive short-pulse light mainly inactivates photosystem I in sunflower leaves. In *Plant and Cell Physiology* 55 (6), pp. 1184–1193. DOI: 10.1093/pcp/pcu061.

Sharma, P.; Jha, A. B.; Dubey, R. S.; Pessarakli, M. (2012): Reactive Oxygen Species, Oxidative Damage, and Antioxidative Defense Mechanism in Plants under Stressful Conditions. In *2090-0120* 2012 (1), pp. 1–26. DOI: 10.1155/2012/217037.

Shimakawa, G.; Kohara, A.; Miyake, C. (2020): Characterization of Light-Enhanced Respiration in Cyanobacteria. In *International journal of molecular sciences* 22 (1). DOI: 10.3390/ijms22010342.

Sonoike, K. (1996): Photoinhibition of Photosystem I: Its Physiological Significance in the Chilling Sensitivity of Plants. In *Plant and Cell Physiology* 37 (3), pp. 239–247. DOI: 10.1093/OXFORDJOURNALS.PCP.A028938.

Sonoike, K. (2011): Photoinhibition of photosystem I. In *Physiologia Plantarum* 142 (1), pp. 56–64. DOI: 10.1111/j.1399-3054.2010.01437.x.

Stern, K. R.; Uno, G. (2005): Introductory plant biology. Princeton, N.J.: Recording for the Blind & Dyslexic.

Suorsa, M.; Järvi, S.; Grieco, M.; Nurmi, M.; Pietrzykowska, M.; Rantala, M. et al. (2012): PROTON GRADIENT REGULATION5 is essential for proper acclimation of *Arabidopsis* photosystem I to naturally and artificially fluctuating light conditions. In *The Plant Cell* 24 (7), pp. 2934–2948. DOI: 10.1105/tpc.112.097162.

Tikhonov, A. N. (2014): The cytochrome b6f complex at the crossroad of photosynthetic electron transport pathways. In *Plant physiology and biochemistry : PPB* 81, pp. 163–183. DOI: 10.1016/j.plaphy.2013.12.011.

Tikkanen, M.; Grebe, S. (2018): Switching off photoprotection of photosystem I - a novel tool for gradual PSI photoinhibition. In *Physiologia Plantarum* 162 (2), pp. 156–161. DOI: 10.1111/ppl.12618.

Tiwari, A.; Mamedov, F.; Grieco, M.; Suorsa, M.; Jajoo, A.; Styring, S. et al. (2016): Photodamage of iron-sulphur clusters in photosystem I induces non-photochemical energy dissipation. In *Nature Plants* 2 (4), p. 16035. DOI: 10.1038/nplants.2016.35.

Tyystjärvi, E.; Aro, E. M. (1996): The rate constant of photoinhibition, measured in lincomycin-treated leaves, is directly proportional to light intensity. In *Proceedings of the National Academy of Sciences of the United States of America* 93 (5), pp. 2213–2218. DOI: 10.1073/pnas.93.5.2213.

Went, N.; Di Marcello, M.; Gnaiger, E. (2021): Oxygen dependence of photosynthesis and light-enhanced dark respiration studied by High-Resolution PhotoRespirometry. With assistance of Erich Gnaiger.

Xue, X.; Gauthier, D. A.; Turpin, D. H.; Weger, H. G. (1996): Interactions between Photosynthesis and Respiration in the Green Alga *Chlamydomonas reinhardtii* (Characterization of Light-Enhanced Dark Respiration). In *Plant Physiology* 112 (3), pp. 1005–1014. DOI: 10.1104/pp.112.3.1005.

Yépez, V.; Kremer, L. S.; Iuso, A.; Gusic, M.; Kopajtich, R.; Koňaříková, E. et al. (2018): OCR-Stats: Robust estimation and statistical testing of mitochondrial respiration activities using Seahorse XF Analyzer. In *PloS one* 13 (7), e0199938. DOI: 10.1371/journal.pone.0199938.

Zolla, L.; Rinalducci, S. (2002): Involvement of active oxygen species in degradation of light-harvesting proteins under light stresses. In *Biochemistry* 41 (48), pp. 14391–14402. DOI: 10.1021/bi0265776.

List of figures

List of tables

List of abbreviations

abbreviation	meaning	unit
O2k	Oxygraph2k	-
NextGen-O2k	next generation of Oxygraph2k	-
PB-Module	O2k-PhotoBiology-Module	-
c_{O_2}	oxygen concentration	µM
d	dilution factor	-
$\bar{x}$	average	
O_2	oxygen	µM
CO_2	carbondioxide	µM
LEDR	light-enhanced dark respiration	$amol \cdot s^1 \cdot x^1$
LEPR	light-enhanced photorespiration	$amol \cdot s^1 \cdot x^1$
NP	net photosynthesis	$amol \cdot s^1 \cdot x^1$
DR	dark respiration	$amol \cdot s^1 \cdot x^1$
ROS	reactive oxygen species	µM
AOX	alternative oxidase	-
G1	group 1	
G2	group 2	
G3	group 3	
$V_{ce,s}$	volume of culture sample	mL
$V_{TRIS,SBC}$	volume of TRIS medium enriched with CO_2	mL
H_2O_2	hydrogen peroxide	µM
O_2^-	superoxide anion radical	µM
$\cdot OH$	hydroxyl radical	µM
PS I	photosystem I	-
PS II	photosystem II	-
J_{O_2}	O_2 flux per volume	$pmol \cdot s^{-1} \cdot mL^{-1}$
I_{O_2}	O_2 flow per cell	$amol \cdot s^1 \cdot x^1$
$C_{ce,s}$	cell-count concentration of culture sample	mM
C_{SBC}	cell-count concentration of sodium bicarbonate	mM
Dp	data points	-
N	technical repeats	-
N	experimental replica	-
n_{SBC}	amount of substance of sodium bicarbonate	mmol
V_{G3}	volume of dilution group 3	mL
m_{SBC}	mass of sodiumbicarbonate	mg
M_{SBC}	molecular mass of sodiumbicarbonate	$mg \cdot mmol^{-1}$
$^1O_2$	singlet oxygen	µM
ATP	adenosine triphosphate	µM
rpm	rotations per minute	
g	gravitational acceleration	$9.81 \ m \cdot s^{-2}$

Supplement

Oxygen dependence of photosynthesis and light-enhanced dark respiration studied by High-Resolution PhotoRespirometry

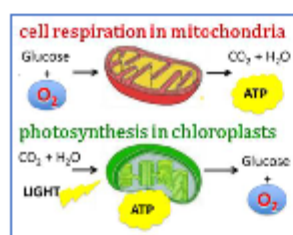Nora Went[1,2], Marco Di Marcello[1], Erich Gnaiger[1,3]*

[1]Oroboros Instruments, Innsbruck, Austria; [2]MCI Management Centre Innsbruck, Austria; [3]Dept Visceral, Transplant and Thoracic Surgery, D Swarovski Research Laboratory, Medical Univ Innsbruck, Austria

* Corresponding author: erich.gnaiger@oroboros.at

Posted Online 2021-04-30

Abstract

The bioenergetic crosstalk between mitochondria and chloroplasts plays a key role in maintaining metabolic integrity and controlling metabolite production for growth and regulation of cell concentration. Dark respiration and photosynthesis were measured in the green alga *Chlamydomonas reinhardtii* at varying oxygen concentrations and three cell concentrations using the NextGen-O2k with the PhotoBiology Module. Maximum net photosynthesis at a light intensity of 350 $\mu mol \cdot s^{-1} \cdot m^{-2}$ (blue light) was inhibited at hyperoxia by 40 % at oxygen concentrations of 550 to 650 μM. Light-enhanced dark respiration reached a (negative) maximum within 30 to 60 s after light-dark transitions and was 3.5- to 4-fold higher than steady-state dark respiration independent of O_2 concentration in the range of 200 to 650 μM.

Keywords – high-resolution respirometry, photosynthesis, dark respiration, *Chlamydomonas reinhardtii*

High-Resolution PhotoRespirometry and cell culture

High-resolution respirometry based on the Oroboros O2k is extensively applied to the study of mitochondrial physiology in the biomedical field [1,2]. Real-time oxygen flux was measured using the NextGen-O2k, a two-chamber instrument, in growth medium TRIS at 25 °C. Light intensities (blue) were controlled with the PhotoBiology-Module in the range from 0 to 350 $\mu mol \cdot s^{-1} \cdot m^{-2}$ (Figure 1). Data were recorded by DatLab 7.4.

Algae were grown photoautotrophically in growth medium TRIS (N- and P-nutrient replete) at 25 °C and a light intensity of 100 $\mu mol \cdot s^{-1} \cdot m^{-2}$ (16:8 h L:D) [3]. Six cultures (*N*=6) were harvested by centrifugation at 1000 *g* (10 min) and diluted in TRIS.